Electronic Supplementary Information

Fabrication of Hierarchical Silica Films with Coexisting Microscale Cracks and Mesopores Enabled by Chlorine-Containing Silica Particle Incorporation

Reo Kimura [a, b], Sunao Chatani [c], Aoi Endo [a, b],
Kurisu Mikami [c], Satoshi Motozuka [d], Kento Takayama [a], Motohiro Tagaya [a, *]

[a] *Department of Materials Science and Bioengineering, Graduate School of Engineering, Nagaoka University of Technology, 1603-1 Kamitomioka, Nagaoka, Niigata 940-2188, Japan.*

[b] *Japan Society for the Promotion of Science (JSPS) Research Fellowship for Young Scientists (DC), 5-3-1 Koji-machi, Chiyoda-ku, Tokyo 102-0083, Japan.*

[c] *Production Department, Ohara Quartz, 1850 Minato, Wakayama, Wakayama 640-8404, Japan*

[d] *Department of Materials Science and Engineering, Kyushu Institute of Technology, 1-1 Sensuicho, Tobata-ku, Kitakyushu 804-8550, Japan*

*** Author to whom correspondence should be addressed:**
Tel: +81-258-47-9345; Fax: +81-258-47-9300, E-mail: tagaya@mst.nagaokaut.ac.jp

Experimental Procedure S1

Porous synthetic quartz glass (porous base material) was obtained at OHARA QUARTZ Corporation using silicon tetrachloride through a thorough hydrolysis reaction in a mixed atmosphere of oxygen and hydrogen flame by the VAD (Vapor Axial Deposition) method. In the process of forming porous base material using the VAD method, silicon tetrachloride was introduced from the centre of an oxygen and hydrogen flame burner, with a flame temperature zone exceeding 1000 °C, extending over a length of 400 mm, and maintaining a hydrogen-to-oxygen volume ratio (H_2/O_2) of 1.5. Then, the chlorine-containing treatment was conducted by applying the silicon tetrachloride gas to the heat treatment atmosphere of the generated porous matrix based on the chemical reactions. This was carried out by heat treatment at 900–1200 °C for 10–40 h in an inert gas atmosphere containing silicon tetrachloride. In this process, the waste particles obtained by scraping the surface of the generated quartz glass were used in this study. Specifically, the particles from the glass containing a higher concentration of chlorine source by silicon tetrachloride gas were named CS.[S1]

CS exhibited amorphous and spherical particles, and the average particle diameters of CS was 143 nm. CS were non-porous, and the chlorine concentration was 0.40 mol%. The surface silanol group fraction of the particles, which was measured via XPS, of CS was 85%.[S2]

References

S1 R. Kimura, S. Chatani, M. Inui, S. Motozuka, Z. Liu, and M. Tagaya, ***Langmuir***, 2024, 40, 8939–8949.

S2 R. Kimura, S. Chatani, M. Inui, S. Motozuka, I. Yamada, and M. Tagaya, ***Nanomaterials***, 2024, 14, 741.

Experimental Procedure S2

A polyamic acid (PAA) solution was spin-coated onto UV-ozone-treated glass (24 × 24 mm^2), followed by drying and baking to obtain polyimide (PI) films. The resulting polyimide (PI) films were subjected to rubbing treatment along the rubbing direction (*R.D.*). A rayon rubbing cloth (filament length: 1.8 mm, 32,000 filaments·cm^{-2}) was used for the rubbing process. The pile penetration depth was defined as the distance from the point at which the deformed filaments were pressed against the surface of the substrate. The contact distance between the filament tops and the substrate surface was fixed at 0.1 mm. The rubbing treatment was performed at a rotation speed of 600 rpm and stage translation speed of 15 mms^{-1}, and the process was repeated four times for each sample.

The MPS precursor solutions were prepared by mixing tetraethoxysilane (TEOS), ultrapure water, ethanol, HCl, P123, and Brij 56 at a molar ratio of (TEOS) 1: (ultrapure water) 1.5: (ethanol) 4: (HCl) 6×10^{-3}: (P123) 9×10^{-3}: (Brij 56) 2.7×10^{-2}. Then, the prepared precursor solutions were spin-coated on the rubbing-treated PI film at 6000 rpm, followed by drying at 40 °C for 18 h and calcination at 350 °C for 6 h to remove P123 and Brij 56 micelles to obtain OMPS [S3].

Reference

S3 Y. Chai, Y. Maruko, Z. Liu, and M. Tagaya, ***J. Mater. Chem. B.***, 2021, 9, 2054–2065.

Experimental Procedure S3

The X-ray diffraction (XRD) patterns were recorded with a horizontal X-ray diffractometer (H-XRD, Smart Lab 9kW, Rigaku Co., Ltd.) with an X-ray source of CuK*α* line (*λ* = 0.15418 nm) and a voltage/current of 45 kV/200 mA. The pore structures of films were evaluated by *out-of-plane* and *in-plane* XRD patterns and *in-plane* XRD *φ*-scan. In detail, the *out-of-plane* XRD patterns were measured, the incident angle (*ω*) and reflection angle (2*θ*) of the X-ray were changed to measure the lattice plane parallel to the film surface (2*θ*/*ω*-scan). The degree of 2*θ* was changed in the range of 0.5–10°. The *d*-spacings (d_{01} (nm) and d_{02} (nm)) were calculated by the Bragg equation (**Eq. S1**).

$$2dsin\theta = n\lambda \qquad \textbf{(Eq. S1)}$$

Out-of-plane, *in-plane*, and *φ*-scan analyses were performed. In the *φ*-scan measurements, the sample was scanned over a range of −180° to 180°, and the full width at half maximum (FWHM, *W*) of the diffraction peak was determined at −90° and 90° (perpendicular to the *R.D.*). These values were substituted into the orientation degree equation to evaluate the degree of orientation of the fibers.

The *in-plane* XRD patterns were measured, where *ω* was fixed at 0.2°, and the 2*θχ* axis was changed to measure the lattice plane perpendicular to the film surface (2*θχ*/*φ*-scan). The degree of 2*θχ* was changed in the range of 0.5–5°. Moreover, the films were set up in the equipment and adjusted so that the X-ray incident directions were almost parallel or perpendicular to the *R.D*. over the incident angle of *ω*. The software of PDXL (Rigaku Co., Ltd.) was used for the calculation of diffraction peak areas. The *in-plane* XRD *φ*-scan profiles were measured where *ω* was fixed at 0.2°, and the 2*θχ* axis was changed in the range between −180 and 180°. When the 2*θχ* axis was changed at −180, 0, and 180°, the direction of the incident X-ray was parallel to the *R.D*. Here, the average half-widths (*W* (degree)) of the diffraction peaks were calculated, which were obtained from the *in-plane* XRD *φ*-scan measurement. Then, the orientation degree (%) was also calculated by **Eq S2**.

$$Orientation\ degree\ (\%) = \frac{(180 - W)}{180} \times 100 \qquad \textbf{(Eq S2)}$$

Experimental Procedure S4

Based on the previous report,[S4] the Brunauer-Emmett-Teller (BET) specific surface area of the samples was calculated using the N_2 adsorption/desorption isotherms. Before the measurement, pretreatment was performed by vacuum heating at 120 °C for 1.5 h using the pretreatment device (Microtrac Bell Corporation, BELSORPvac II). The BET specific surface area (S_{BET} $m^2 \cdot g^{-1}$) was calculated using the equation (**Eq. S5**), with the adsorption amount (V_m $cm^3 \cdot (S.T.P) \cdot g^{-1}$) when the sample surface was covered with the N_2 monolayer adsorption and the cross-sectional N_2 molecular occupation (S m^2). N_A represents Avogadro's constant (6.02214×10^{23} mol^{-1}). V_m represents the adsorption amount per unit mass converted to standard conditions.

	$S_{BET} = \frac{V_m}{22414} \times N_A \times S$	(**Eq. S5**)

The BET method is based on the Langmuir monolayer adsorption theory, which is extended to monolayer adsorption, as demonstrated in the equation.[S5] Here, P represents the pressure, P_0 is the saturated vapor pressure, V is the total gas adsorption amount, and C is the BET constant. By obtaining the adsorption amount (V_a) at a certain relative pressure from the actual adsorption isotherm and plotting $P \cdot P_0^{-1}$ on the horizontal axis and $P/(P_0 - P)V_a$ on the vertical axis, a straight line is obtained with a slope of $((C-1)/(V_m \cdot C))$ and an intercept of $(1/(V_m \cdot C))$. This graph is referred to as the BET plot, and S_{BET} can be determined by substituting the obtained V_m into the equation (**Eq S6**).

$$\frac{P}{V_a(P_0 - P)} = \frac{1}{V_m \times C} + \left(\frac{C-1}{V_m \times C}\right)\left(\frac{P}{P_0}\right) \quad \text{(Eq S6)}$$

References

S4 S. Brunauer, P.H. Emmett, and E. Teller*, J. Am. Chem. Soc*, 1938, **60**, 309–319.

S5 I. Langmuir*, J. Am. Chem.Soc*, 1918, **40**, 1361–1403.

Experimental Procedure S5

The Barrett–Joyner–Halenda (BJH) pore size distribution was calculated based on the capillary condensation theory (Kelvin equation; **Eq. S7**).[S6]

$$r_k = r_p - t = \frac{-2\sigma V \cos\theta}{RT \ln(P/P_0)} \quad \textbf{(Eq. S7)}$$

The BJH method is effective for evaluating the pore size distribution in the mesopore range (2–50 nm). Here, $r_p$represents the pore radius, $r_k$denotes the radius of the pore where capillary condensation occurs, and t represents the thickness of the multilayer adsorbed film. In addition, σ and θ represent the surface tension and contact angle, respectively. When the cylindrical length of pores with radii between $r$and $r + dr$is expressed as $L(r)dr$, the mass balance at a given relative pressure can be described by **Eq. S8**.

$$V - V_x = \int_{rp}^{\infty} \pi (r - t)^2 L(r) dr \quad \textbf{(Eq. S8)}$$

Here, Vrepresents the total pore volume and $V_x$represents the adsorption amount at a given relative pressure. The difference between $V$and $V_x$corresponds to the total pore space where the capillary condensation has not occurred at that relative pressure. Since $V$and $V_x$are experimentally obtained values, the pore size distribution $L(r)$ can be determined, and its maximum value was defined as the BJH pore radius (r_{BJH}). Furthermore, the pore volume V_p(m³) was calculated from the obtained $r_{BJH}$and S_{BET} using **Eq. S9**. BJH pore size distribution calculated based on the adsorption branch of the isotherm.

$$V_p = \frac{{S_{BET}}^2}{2\pi r_{BJH}} V \quad \textbf{(Eq. S9)}$$

Reference

S6 E.P. Barrett, L.G. Joyner, P.P. Halenda, ***J. Am. Chem. Soc.,*** 73 (1951) 373–380.

Fig. S1

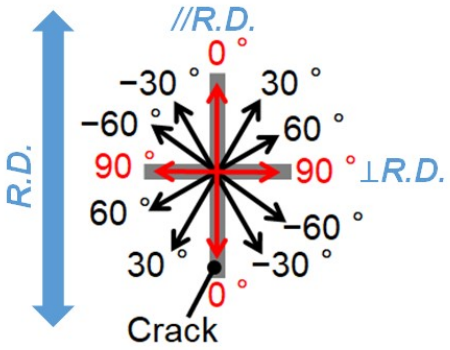

Fig. S1. Calculation method of crack orientation distributions on the films.

Fig. S2

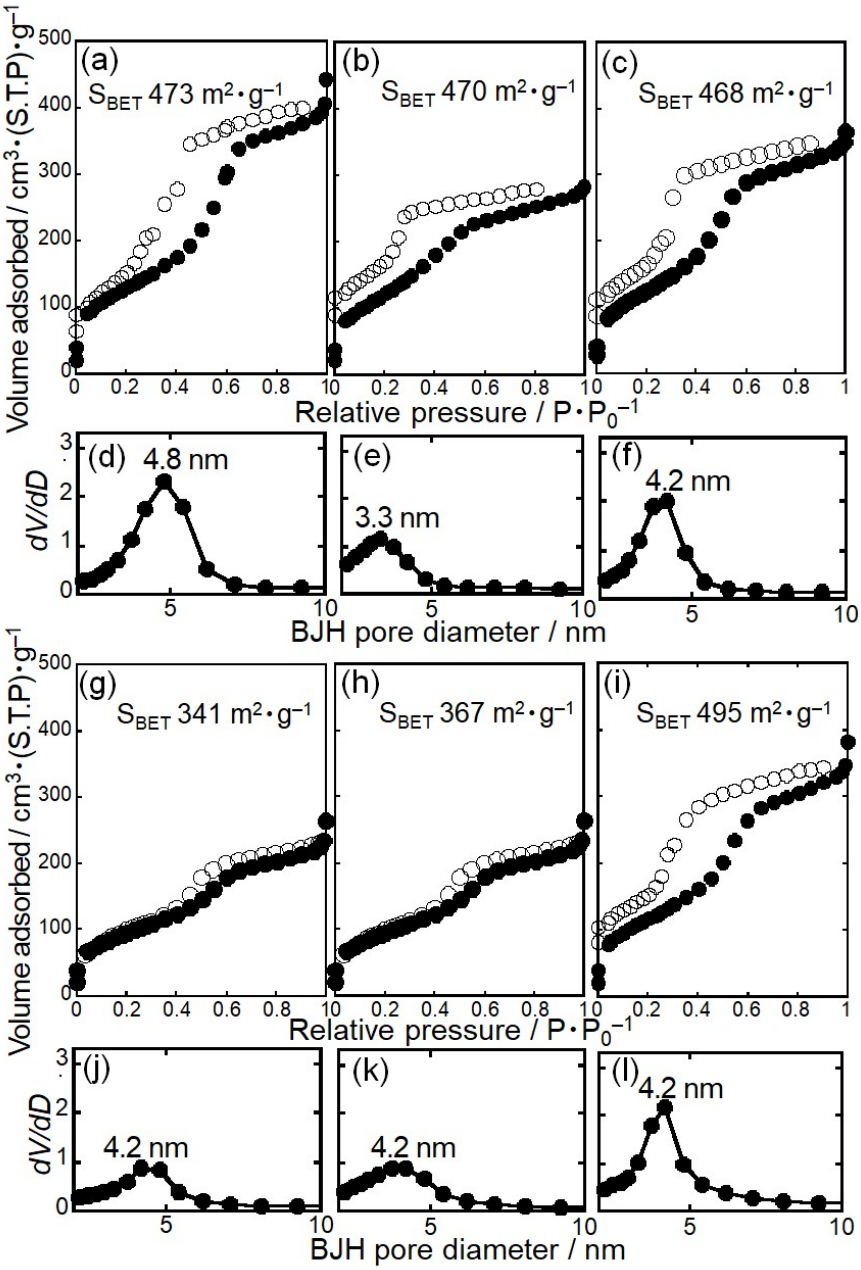

Fig. S2. (a, b, c, g, h, i) N_2 adsorption (close marks) and desorption (open marks) isotherms, and (d, e, f, j, k, l) BJH pore size distributions of (a, d) **0**CSMPS, (b, e) **0.05**CSMPS, (c, f) **0.1**CSMPS, (g, j) **0.5**CSMPS, (h, k) **1**CSMPS, and (i, l) **1**CSMPS-**Ref**, respectively.

Fig. S3

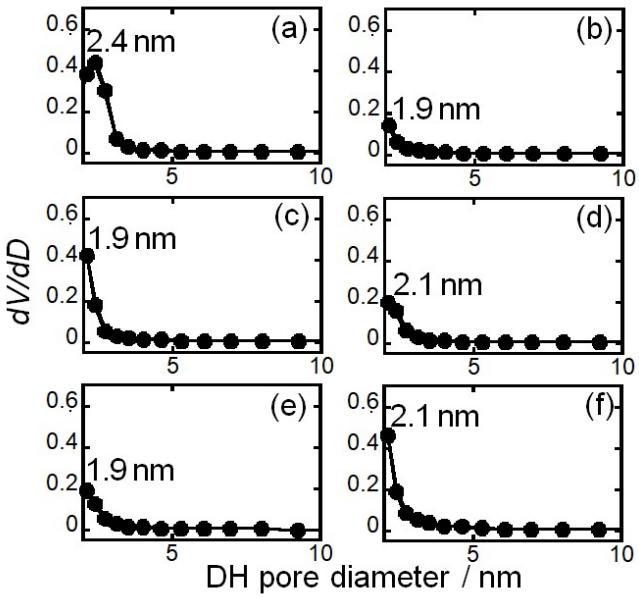

Fig. S3. DH pore size distributions of (a) **0**CSMPS, (b) **0.05**CSMPS, (c) **0.1**CSMPS, (d) **0.5**CSMPS, (e) **1**CSMPS, and (f) **1**CSMPS-**Ref**, respectively.

Fig. S4

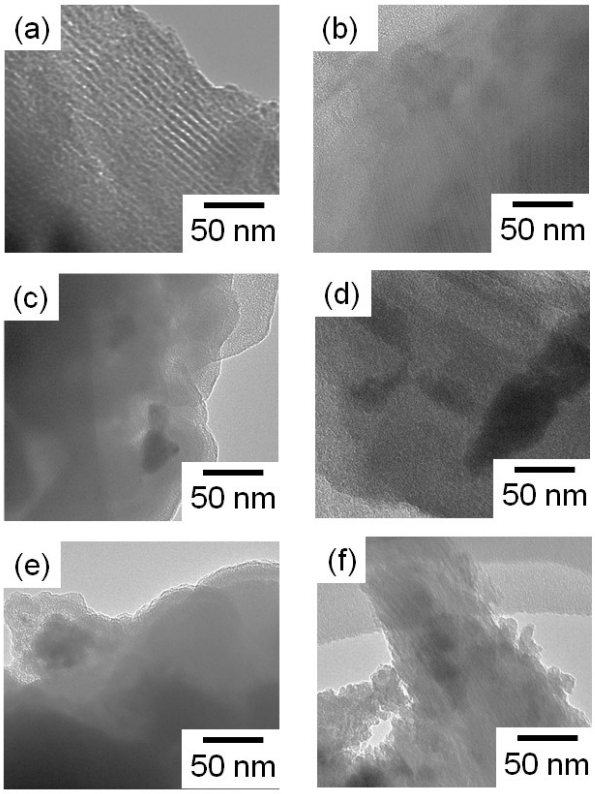

Fig. S4. TEM images of the scraped surfaces of (a) **0**CSMPS, (b) **0.05**CSMPS, (c) **0.1**CSMPS, (d) **0.5**CSMPS, (e) **1**CSMPS, and (f) **1**CSMPS-**Ref**, respectively.